



Effect of Water Depth on ROV Materials Selection and Designs

OLUSEGUN, Samuel Dare^a and OGBE, Emmanuel Ediba^b

^{ab}Department of Marine Engineering, Nigeria Maritime University Okerenkoko, Delta State, Nigeria.

ABSTRACT

The aim of this research is to select ROV Frame Material for Improved Performance in Varying Ocean Depth with the aid of MATLAB programming language and STAAD.Pro software by applying the numerical skills. This was achieved by first running a material test analysis on the frame of the ROV, then a stress analysis test is carried out on the material and sizes selected to determine if the ROV frame can withstand the stress on the material. The total force due to wave effect and total forces on the ROV is then computed using the MATLAB, then the power required to drive the ROV at different water depth of 50m, 500m and 1000m during the operation is computed. Based on the results, suitable material among the under study is selected. It can be deduced from the results that, the maximum internal displacement of the ROV frame that houses all the components is able to withstand over 50 kPa with an inner displacement of 5mm. The result when compared with the maximum allowable stress of steel of 210 *Gpa* was found to be satisfactory. The von mises stress of the ROV frame under load which is the value used to determine if a given material will yield or fracture under load was also computed during the ROV design. The von mises stress helps to show if the material will fail under the different impacted load on the ROV frame based on the nodal sub-region employ, and the areas or region with least impacted load as shown with blue coloration having a von mises stress less than 200.4665 kpa while the area or region with the most load impact or distribution is shown with red coloration with maximum von mises stress greater than or equal to 53.936212 Mpa. The design also computes the power required to drive the ROV and the power that will be require to drive the ROV though the maximum power of about 2000kw as the working power of the ROV. It was also observed that the minimum drive power of the ROV (250kw) was recorded at 1000m water depth. The task to determine how deep into ocean the Remotely Operated Underwater Vehicle can dive while maintaining a safety factor of 1.5 was also accomplish as Stainless steel 317, Titanium Grade 5 and Aluminium 7075 meet the factor of safety condition at water depth of 1000m.

Keyword: ROV Frame Material; Ocean Depth; Maximum Allowable Stress; Von Mises Stress; Stainless Steel; Titanium; Aluminium; Factor of Safety

1.INTRODUCTION

Subsea production relies on the on-time delivery of maintenance services on subsea assets using ROVs (remotely operated vehicles) and other specialised tools. These services are normally outsourced to specialist companies which have the expertise as well as specialist tools and methods. These maintenance activities are undertaken on subsea production systems (well heads, manifolds, flow-line, risers, etc.) to preserve or restore their integrity. They are quick response and of relatively short duration. They cover light construction activities such as tie-ins and leak clamps. The industry categorises these activities into three groups: Inspections, Maintenance and Repair. Inspections are executed with ROV carrying appropriate NDT tools. These are statutory and run on five year's cycle. Maintenance activities include the replacement of items such as control modules as well as the regular cleaning and clearing of subsea assets. These are recurring, standardised and provide information for the program of repairs. Such Repair job-types tend to be job-specific and include restorations and modifications. They require substantial Engineering input. The industry acronym of IMR (or the equivalent IRM) appears to be an attempt to integrate these service lines on one vessel Roy, (1998).

Today, massive remotely operated vehicles (ROVs) probe the ocean depths worldwide. Even the deepest point in the ocean, the Mariana Trench, has seen the footprint of an ROV – Japan's Kaiko. But the complex work vehicles that populate the offshore drilling platforms and ships are not the only systems that have come of age through the advancement of technology; the observation class ROVs (OCROVs)—generally portable ROVs that weigh less than 200 lbs (91 kg)—have taken the technological advancements and the miniaturization of electronics and camera systems and applied them to an ever-increasing array of missions. Missions such as body recovery, dam inspections, nuclear inspections, treasure hunting, archeology, fish assessment, ship husbandry and more recently homeland security have become routine for OCROVs. No longer are observation vehicles an expensive addition to a dive company's tool bag; they have become a necessity, keeping divers out of hazardous situations or conditions and allowing the small vehicles to enter underwater locations too confining for a diver Salleh, (2008).

But advancements in technology can also increase complexity and cost. While many OCROV developers are marketing increasingly complex systems, others are returning to the days of the “flying eyeball.” Regardless of a company’s design philosophy, OCROVs have come of age.

Work class remotely operated vehicle (ROV) support is found to be highly essential in the oil and gas sector, deep water research, and offshore energy sectors (Roy, 1998) where the oil and gas sector is accountable for 75% of ROV usage in drilling, exploration and subsea infrastructural developments Salleh, (2008). The global annual expenditure on work class ROV operations is set to increase from \$1.6 billion in 2013 to \$2.4 billion in 2017, a compounded annual growth rate of 11.3% Roy, (1998). The world fleet of work class ROVs has grown from 641 units in 2011 (Symes, 2013) to 1102 units in 2013 Henri, et al. (2010). This is largely due to the move toward deeper waters and more complicated offshore field development programs Vedachalam, et al. (2013); Smith, & Simpson, (2010); International Electro technical Commission, (2003); International Standard, (2003). The essential use of work class ROV in deeper water was clearly demonstrated during the Macondo well head blow-out in the Gulf of Mexico (Manecius, et al., 2010) which demanded safe and reliable operation in the challenging environment. This demands the need for relevant safety standards and procedures to be implemented in the fast-growing subsea intervention industry, where the vehicle risk tolerance levels and associated safety requirements are dictated by the mission for which the vehicle operations are called. The required safety levels for the intervention system are normally dictated by the Health, Safety and Environmental (HSE) regulations already in place which is usually described by the safety integrity levels (SIL) based on IEC 61508 and 61511 standards (Amudha, et al., 2009); (Ramesh, et al., 2010); (Ahmed, et al., 2014) and the operational SIL of the ROV needs to be in compliant with the required SIL. Thus, a quantitative, risk based, operation specific assessment of the vehicle’s SIL is required, so as to ensure confidence in the use of ROV for the specific operation. Even though, safety assessment by qualitative methods for the required safety levels in offshore environments (Guangyi, et al., 2018) and surface vessels (Hasan, et al., 2018) exist, such methods are seldom practiced in the ROV industry where safety assessment has a high level of uncertainty due to the insufficient reported failure data which has been a major concern for risk related decision support. Novel decision-making techniques are required to make the design and operation decisions efficiently and in the absence of which, it might be difficult to compare the design costs and operational benefits. Thus, the need for suitable risk assessment and quantitative safety models based on HSE are required. The CAPEX and OPEX of the ROV are decided by the frequency of maintenance required to upkeep the SIL. Thus, the maintenance expenditure could be greatly reduced by safety centered design practices. This paper presents an approach to the operational safety modeling and estimation of SIL for deep water electric work class ROV, with reference to the ROSUB 6000 designed by the National Institute of Ocean Technology (NIOT).

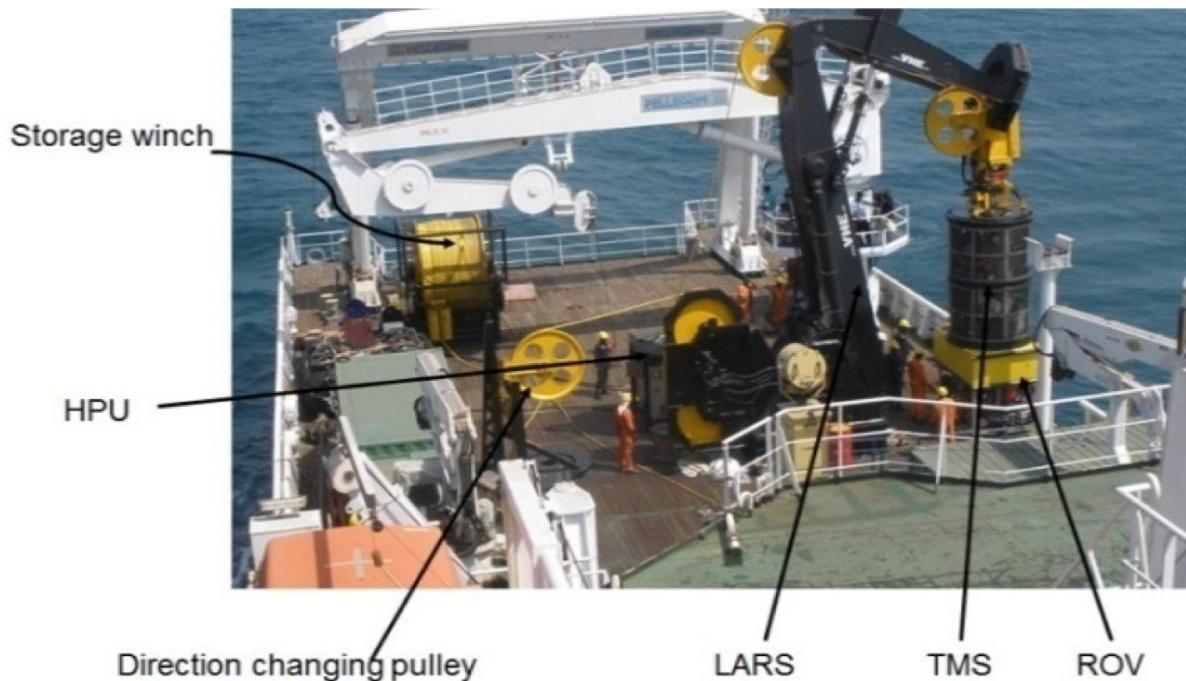


Figure 1: General Lunching of a Remotely Operated Vehicle

II. METHODOLOGY

2.1 Force Estimation at Different Water Depth

2.1.1 Wave length

Wave length is a measure of distance between two identical peaks, that is high points or low points in a wave.

$$\lambda_0 = \frac{g}{2 \times \pi} \times T^2 \quad (1)$$

λ_0 The water wave length at deep sea

g The acceleration due to gravity

T The wave period

So test to determine water

$$\frac{d}{\lambda_0} \text{ is } > \frac{1}{2}$$

it means deep water

$$\lambda = \lambda_0$$

But,

If $\frac{1}{2}$ is $< \frac{d}{\lambda_0} \geq \frac{1}{20}$ it means transitional water

And trial and error method is use

$$\lambda_n = \frac{(g \times T^2)}{2 \times \pi} \times \tanh \frac{(2 \times \pi \times d)}{\lambda_{n-1}} \quad (2)$$

d The sea water depth

λ_{n-1} The wave length at the previous trial

λ_n The wave length at the current trial

At each trial the new wave length λ_n should replace the old wave length λ_{n-1} and the trial should stop when error is less than 0.1 percent

$$\text{Error} = \left[\frac{\lambda_n - \lambda_{n-1}}{\lambda_n} \right] \times 100 < 0.1\% \quad (3)$$

Error The error of iteration

Then,

If the Error is less than 0.1%

$$\lambda = \lambda_n \quad (4)$$

λ The final wave length after iterations

Also,

If $\frac{d}{\lambda_0} < \frac{1}{20}$ it means shallow water

The trial and error method used for the transitional water is also applicable

2.1.2 Wave number

The wave number is the spatial frequency of a wave either in cycles per unit wave length or radians per unit wave length.

$$k = \frac{2 \times \pi}{\lambda} \quad (5)$$

k The wave number

2.1.3 Wave frequency

The wave frequency describes the number of waves that pass the fixed offshore structures place at the sea in a given amount of time.

$$w = \sqrt{g \times k \times \tanh(k \times d)} \quad (6)$$

w The wave angular frequency

2.1.4 Wave maximum horizontal velocity

The wave maximum horizontal velocity is that maximum velocity taken as at when the wave angle is maximum on the horizontal plane of the wave.

$$U_{max} = \frac{H_{max} \times T \times g}{2 \times \lambda} \quad (7)$$

U_{max} The wave maximum horizontal velocity

2.1.5 Keulegan-Carpenter number

The Keulegan-Carpenter number is dimensionless quantities which describe the relative importance of the drag forces over inertia forces and vice versa for object in an oscillatory fluid flow, like the water wave.

$$Kc = \frac{U_{max} \times T}{D} \quad (8)$$

Kc The Keulegan-Carpenter number

D The ROV Frame Diameter

2.1.6 Reynolds number

The Reynolds number in the context is the ratio of inertia forces to viscous forces within a fluid in this case wave which is subjected to relative internal movement due to different fluid velocities.

$$Re = \frac{U_{max} \times D}{\nu} \quad (9)$$

Re The Reynolds number

ν The kinematics viscosity of water

2.1.7 Tests for linearity of water wave

Condition of linear wave theory

If $\frac{D}{\lambda} > 0.2$ linear wave theory is not applicable

Also,

If $\frac{D}{\lambda} \leq 0.2$ linear wave theory is applicable

2.1.8 Conditions for drag coefficient and inertia coefficient

For $Kc > 25$ and $Re > 1.5 \times 10^6$

Then, $Cm = 1.8$ and $Cd = 0.62$

If $10^5 < Re < 1.5 \times 10^6$

Then, $Cm = 1.8$ and $Cd = 0.8$

For $5 < Kc < 25$

If $Re > 1.5 \times 10^6$

Then, $Cm = 1.8$ and $Cd = 0.62$

If $Re < 1.5 \times 10^6$

Then, $Cm = 1.8$ and $Cd = 0.62$

For $Kc < 5$

Then, $Cm = 2.0$ and $Cd = 0$

Cm The inertia coefficient

Cd The drag coefficient

Now let calculate some constant associated with the inertia and drag force

2.1.9 Constant of inertia and drag force

These constants of inertia force and drag force are extracts of a high integration computation. Starting with the wave potential through the velocity potential while faction in the Morrison equation and integrate through the entire structure. These constants are used to compute the inertia force and drag force.

2.1.9.1 Constant of inertia force

$$A_1 = \frac{\pi \times D}{4 \times H_{max}} \quad (10)$$

A_1 The constant of inertia force

2.1.9.2 Constant of drag force

$$A_2 = \frac{(2 \times k \times d) + (\sinh(2 \times k \times d))}{16 \times \sinh(k \times d)^2} \quad (11)$$

A_2 The constant of drag force

For different value of phase angle of the water wave say θ

So, For $\theta = 0: 10: 360$

2.1.10 Inertia force

The inertia force depends on the ROV structure own weight material properties, which is a function of the pipe diameter in hollow case and width in frame case.

$$F_m = \frac{D \times \pi \times \rho \times H_{max}^2 \times \lambda}{T^2} \times [A_1 \times Cm \times \sin(\theta)] \quad (12)$$

F_m The inertia force

ρ The sea water density

θ The wave phase angle in degrees

2.1.11 Drag force

The wave drag force is defined by the film of water wave which is a function of the flow velocity, water density and dynamic viscosity.

$$F_d = \frac{D \times \pi \times \rho \times H_{max}^2 \times \lambda}{T^2} \times [(A_2 \times Cd \times |\cos \theta| \times \cos \theta)] \quad (13)$$

F_d The drag wave force

2.1.12 Total wave force

The total wave force is the sum of the inertia force and drag force at different wave angle, this shown the entire force imparted on the offshore structure by the wave at different wave angle under linear water flow.

$$F_T = F_m + F_d \\ = \frac{D \times \pi \times \rho \times H_{max}^2 \times \lambda}{T^2} \times [A_1 \times Cm \times \sin \theta + (A_2 \times Cd \times |\cos \theta| \times \cos \theta)] \quad (14)$$

F_T The total wave force

$$\sigma = \frac{P}{A} \quad (15)$$

The points very near the application of the loads experience a larger stress value whereas, the points far away from it on the same section has lower stress value. The variation of stress across the cross section is negligible when the section considered is far away, about equal to the width of the bar, from the application of point loads. Thus, except in the immediate vicinity of the points where the load is applied, the stress distribution may be assumed to be uniform and is independent of the mode of application of loads.

There are numerous variables that were looked into, for example safety factor, material, thickness, length, and diameter. Due to this, a spreadsheet was made to enter all these parameters, and calculate the maximum depth with the corresponding cost. The unmanned submersible will make out of a barrel lodging all the wires, circuits, and cameras. The failure analysis will be dependent upon this cylinder's behaviour as the depth increases. The joined spreadsheet utilizes the comparisons for hoop stress, longitudinal stress, and axial stress to verify the principle stresses. It then connects the principle stress to the Von Mises comparison to confirm the factor of safety. The previous equations are recorded below. The upcoming analysis depends on a couple of presumptions.

$$\sigma_a = \frac{P \times r}{t} \quad (16)$$

σ_a is Axial Stress and σ_p is the Principal Stress on the Frame

$$\sigma_p = \frac{\sigma_x + \sigma_y}{2} \pm \sqrt{\frac{\sigma_x - \sigma_y}{2}^2 + \tau_{xy}^2} \quad (17)$$

$$\sigma_{vm} = \sqrt{\frac{(\sigma_1 - \sigma_2)^2 + (\sigma_2 - \sigma_3)^2 + (\sigma_3 - \sigma_1)^2}{2}} \quad (18)$$

σ_{vm} is the Von-Mises Stress

2.2.2 Power Required to Drive the ROV

The power required to drive the ROV is the minimum estimated power required to drive the ROV using different water depth. Different material will be required different power to drive the ROV at same depth because the different material is expected to have different self-weight.

$$P = F_T \times U_{max} \quad (19)$$

2.3 Design Parameters

Table 1: Input Parameters to the Matlab Source Code and Solid Works

Parameters Name	Value
ROV Frame Diameter	0.30m
ROV cable Diameter	0.009m
ROV Frame Length	1.5m
ROV Cable Length	1045m
Water Density	$1025 \text{ Kg}/\text{m}^3$
Water Depth	1000m
Kinematic Velocity	$0.00000117 \text{ m}^2/\text{s}^2$
Wave Period	15sec
Significant Wave Height	8m
Wave Frequencies	$0.1 \text{ rad}/\text{s}$ to $5.0 \text{ rad}/\text{s}$
Current Velocity	$1.45 \text{ m}/\text{s}$

Table 1 is the general input to the Matlab source code and solid works and is basically classified into four classes. They are the ROV frame parameter (frame pipe diameter, frame pipe length, cable diameter and cable length), water parameter (water depth, water density and kinematic viscosity), wave parameter (wave period, wave frequencies, significant wave height) and current parameters (water current velocities).

III. RESULTS AND DISCUSSION

3.1 Results

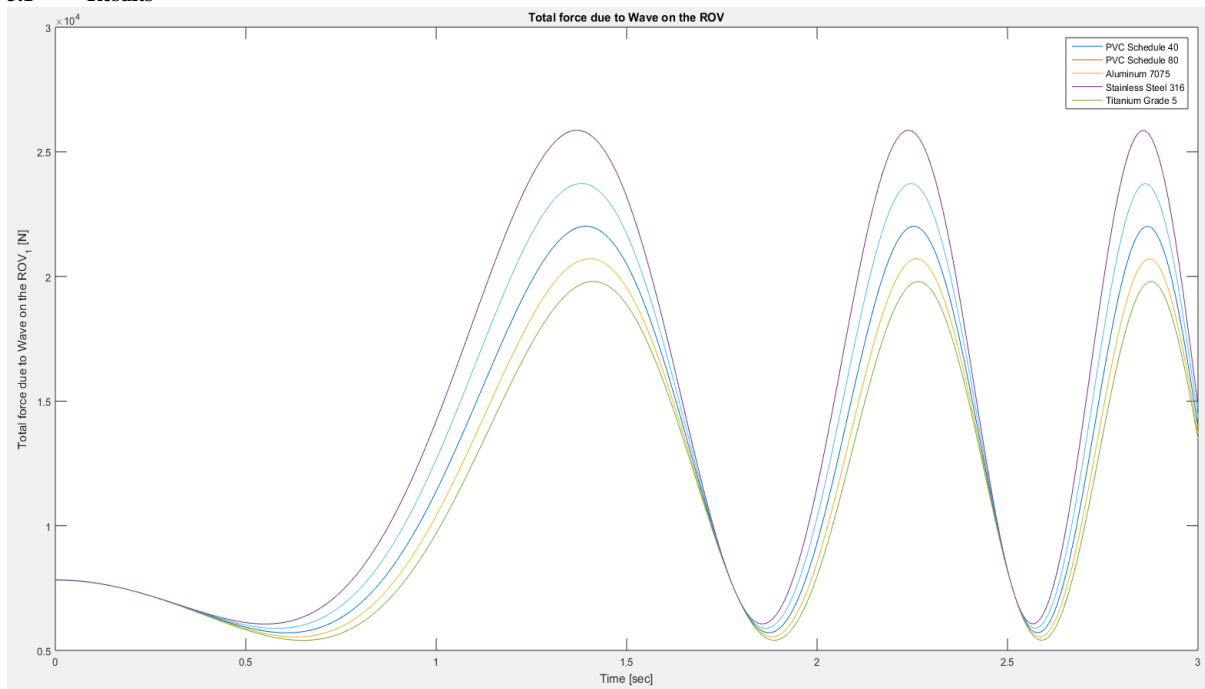


Figure 2: Total Force due to Wave on the ROV at Water Depth 1000m

Figure 2 shows the total force due to wave on the ROV at water depth of 1000m against time. This was done by summing the inertia and drag force on the frame and the cable. The total force due to wave on the ROV start from the near minimum positive at time zero and increases to the positive at time 1.45 sec with total force value of 25000N then the total force begins to reduce again to a minimum positive at time of 1.85 sec with wave force value of 5500N. It was observed that as time progresses the successive crest of wave force on the ROV graph remain same. The total force due to wave effect on the ROV graph follows a typical wave graph with same crest because as time increases the effect of the wave load on the ROV decreases for a regular wave but the self-weight remains the same throughout.

When compared with other water depth (50m and 500m), figure 2 with water depth of 1000m has the highest total force on ROV frame for all the materials. The total force on the ROV frame increases from 11000N for water depth 50m to 11900N for 500m and now 25000N for water depth of 1000m.

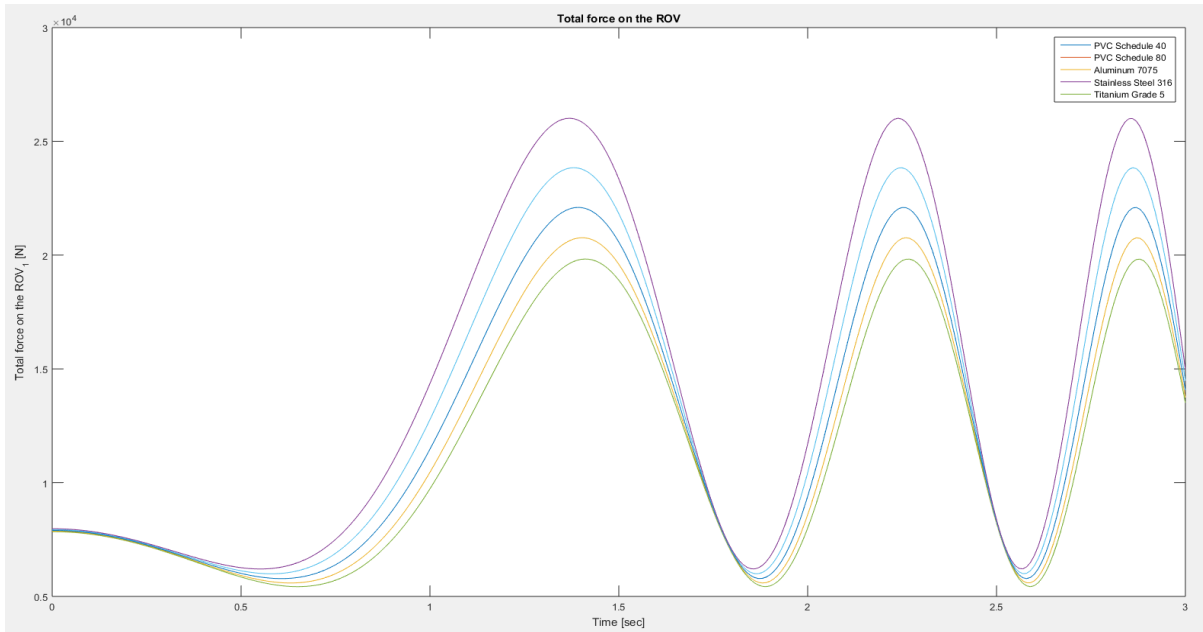


Figure 3: Total Forces on the ROV at Water Depth 1000m

Figure 3 shows the total force on the ROV at water depth of 1000m against time. This was done by summing the total force due to wave effect on the frame and the cable and the force due to water current at 1000m water depth. The total force on the ROV start from the minimum positive at time 0sec and increases to the positive at time 1.45 sec with total force value of 26000N then the total force begins to reduce again to a minimum positive at time of 1.85 sec with total force value of 5600N. It was observed that as time progresses the successive crest of the total force on the ROV graph remain same. The total force on the ROV graph follows a typical wave graph with same crest because as time increases the effect of the wave load on the ROV decreases for a regular wave but the self-weight remains the same throughout.

When compared with other water depth (50m and 500m), figure 3 with water depth of 1000m has the highest total force on ROV frame for all the materials. The total force on the ROV frame increases from 11400N for water depth 50m to 12000N for 500m and now 26000N for water depth of 1000m.

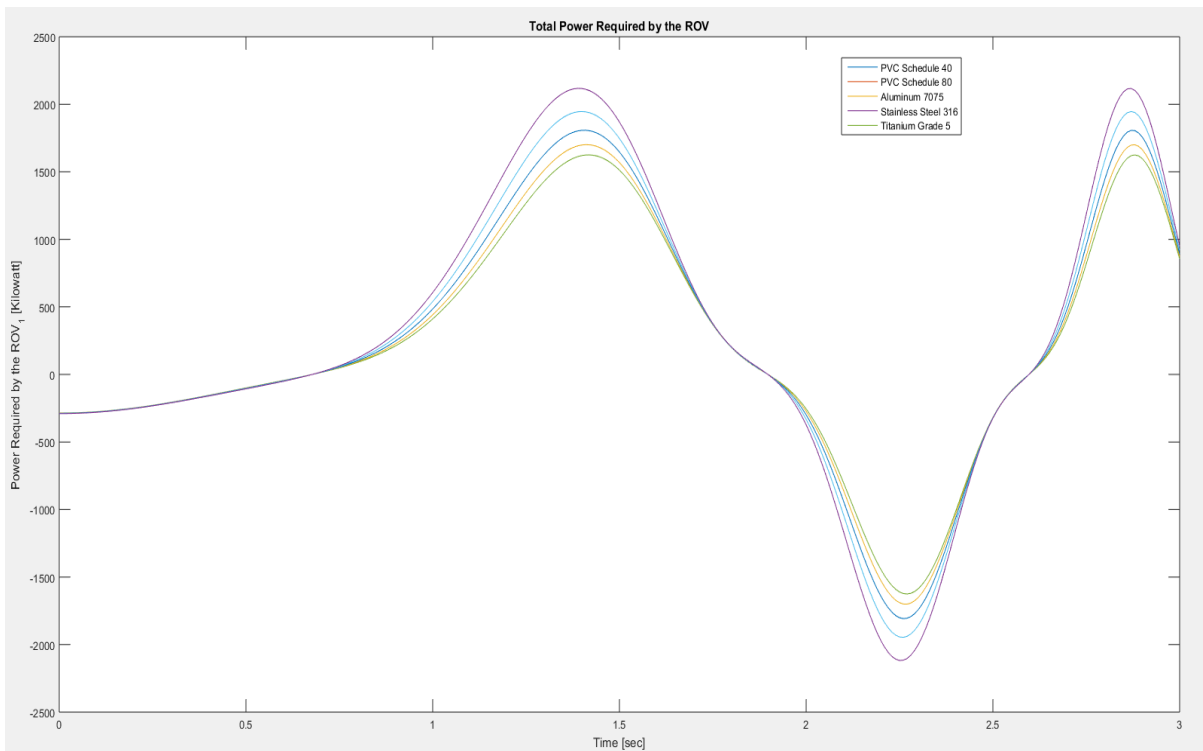


Figure 4: Total Power Required by the ROV at Water Depth 1000m

Figure 4 shows the total power required by the ROV using different material at water depth of 1000m against time. This define the power that will be require to drive the ROV under different material, though the maximum power required by the ROV is about 2000kw for a stainless-steel material while the Titanium grade 5 has the least maximum value of power required to drive the ROV at 2.25 sec. It was also observed from Figure 4that the power required by the ROV start at the minimum point close to zero (250kw) in all the cases of materials under consideration before a gradual increase as time progresses. It was also observed that the power required to drive the ROV tends to remain same in successive crest for all material cases under study as time progresses, which means that for a larger time the power require will definite remain same since the ROV self-weight is constant.

When compared the power required to drive the ROV at 1000m water depth (figure 4). It observed that the power required has increases from 990kw at 50m to 1700kw at 500m, and now 2000kw at 1000m water depth. Also, the stainless-steel material still required the highest power at 1000m when compared with other materials.

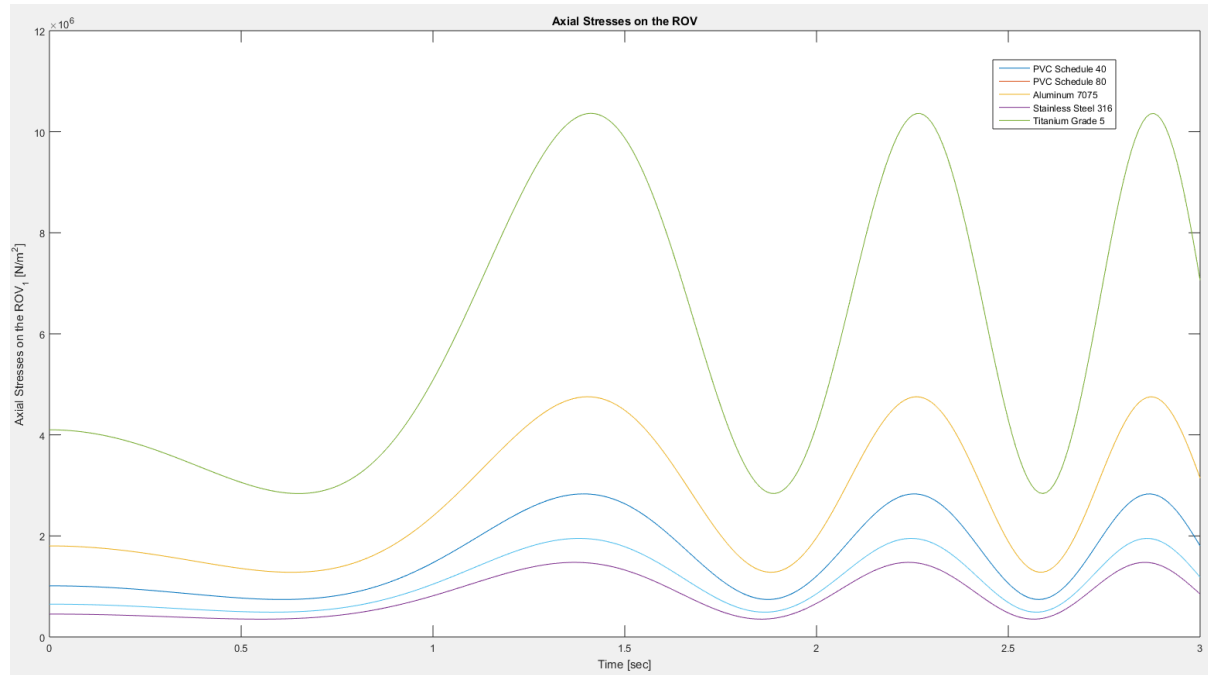


Figure 5: Axial Stresses on the ROV at Water Depth 1000m

Figure 5 shows the axial stresses on the ROV at water depth of 1000m against time, which is the results of a force acting perpendicular to an area of the ROV frame, causing the extension or compression of the material. The axial stress start at the minimum values because the total force on the ROV is also minimum at time of 0sec. The axial stress increases progressively as time increases and comes to the maximum value at 1.4sec with $10.2 \times 10^6 N/m^2$ for Titanium Grade 5 material which has the maximum axial stress when compared with others material and $1.2 \times 10^6 N/m^2$ for stainless-steel which has the minimum axial stress. It was also observed that the axial stresses on the ROV tends to remain same in successive crest for all materials under study as time progresses, due to the fact that the total force on the ROV tend is same pattern.

Figure 5shows that the axial stress on the ROV frame increases with water depth from $4.7 \times 10^6 N/m^2$ to $5.2 \times 10^6 N/m^2$ and $10.2 \times 10^6 N/m^2$ for Titanium Grade 5 and from $0.4 \times 10^6 N/m^2$ to $0.5 \times 10^6 N/m^2$ and $1.2 \times 10^6 N/m^2$ the Stainless-steel material.

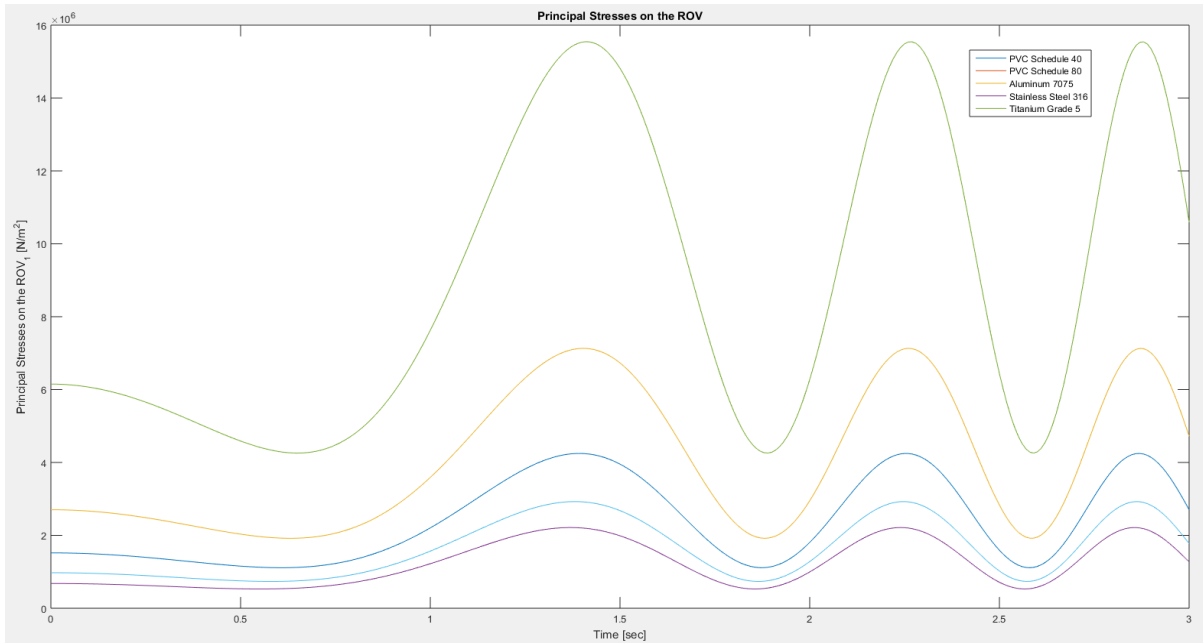


Figure 6: Principal Stresses on the ROV at Water Depth 1000m

Figure 6 shows the principal stresses on the ROV at water depth of 1000m against time. The principal stresses are those stresses acting on the principal plane. The principal stress start at the minimum values because the axial stresses on the ROV for all material is also minimum at time of 0sec. The principal stress increases progressively as time increases and comes to the maximum value at 1.4sec with $15.5 \times 10^6 \text{ N/m}^2$ for Titanium Grade 5 material which has the maximum axial stress when compared with others material and $1.6 \times 10^6 \text{ N/m}^2$ for stainless-steel which has the minimum axial stress. It was also observed that the principal stresses on the ROV tends to remain same in successive crest for all materials under study as time progresses, due to the fact that the axial stress on the ROV tend is same pattern.

Conclusively, when figure 6 was compared, the principal stress on the ROV frame increases with water depth for Titanium Grade 5 ($7.0 \times 10^6 \text{ N/m}^2$ to $7.7 \times 10^6 \text{ N/m}^2$ and $15.5 \times 10^6 \text{ N/m}^2$) and other materials. The Stainless-steel did not experience any significant change between water depth 50m and 500m $0.8 \times 10^6 \text{ N/m}^2$, though the stainless-steel principal stress did increases to $1.6 \times 10^6 \text{ N/m}^2$ at 1000m water depth.

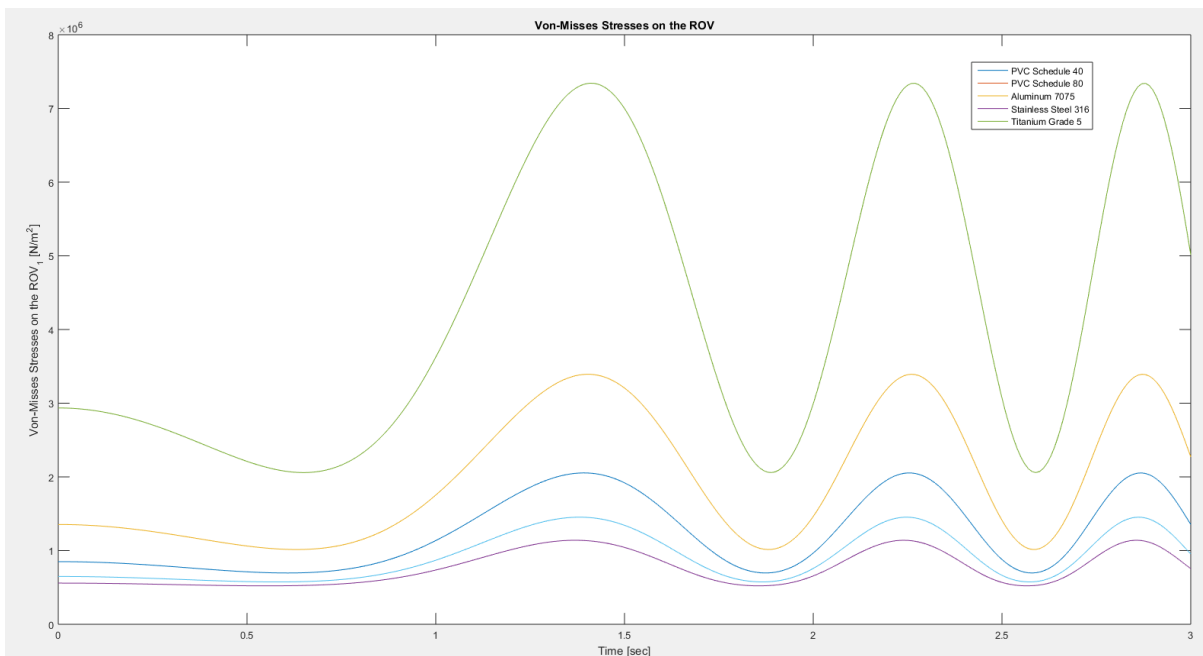


Figure 7: Von-Mises Stresses on the ROV at Water Depth 1000m

Figure 7 shows the principal stresses on the ROV at water depth of 1000m against time. The von-mises stresses of a material under load is equal or greater than the yield limit of the same material under simple tension. The von-mises stress start at the minimum values because the principal stresses on the ROV for all material is also minimum at time of 0sec. The von-mises stress increases progressively as time

increases and comes to the maximum value at 1.4sec with $7.2 \times 10^6 N/m^2$ for Titanium Grade 5 material which has the maximum axial stress when compared with others material and $0.8 \times 10^6 N/m^2$ for stainless-steel which has the minimum axial stress. It was also observed that the von-mises stresses on the ROV tends to remain same in successive crest for all materials under study as time progresses, due to the fact that the axial stress on the ROV tend is same pattern.

Conclusively, when figure 7 was compared, it was observed that the von-mises stress on the ROV frame increases with water depth for Titanium Grade 5 ($3.4 \times 10^6 N/m^2$ to $3.7 \times 10^6 N/m^2$ and to $7.2 \times 10^6 N/m^2$ and other materials. The Stainless-steel did not experience any significant change between water depth 50m and 500m which has von-mises stress of ($0.5 \times 10^6 N/m^2$), though the von-mises stress did increases to $0.8 \times 10^6 N/m^2$ for a stainless-steel material.

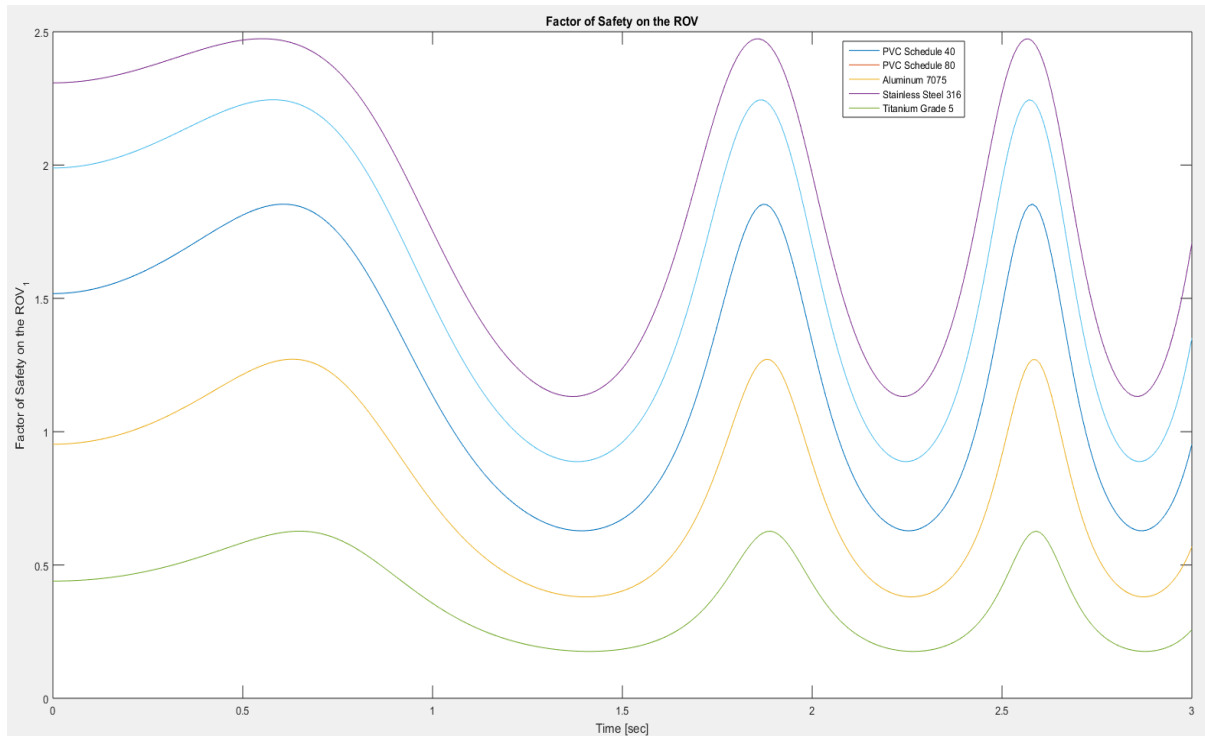


Figure 8: Factor of Safety on the ROV at Water Depth 1000m

Figure 8 shows the factor of safety on the ROV at water depth of 1000m against time. The factor of safety which is the ratio of ultimate stress and working stress of a material under load. The factor of safety unlike the other parameters computed is minimal at maximum total force and maximum at minimum total force. The factor of safety start at the near maximum values because the stresses on the ROV for all material is also near minimum at time of 0sec. The factor of safety increases progressively as time increases and comes to the maximum value at 0.75sec with 0.5 for Titanium Grade 5 material which has the minimum factor of safety when compared with others material and 2.5 for stainless-steel which has the maximum factor of safety. It was also observed that the factor of safety of the ROV tends to remain same in successive crest for all materials under study as time progresses, due to the fact that the axial stress on the ROV tend is same pattern. Conclusively the stainless-steel material is also ideal for water depth of 1000m reason been that it has the minimum axial, principal and von-mises stress than other materials when exposed to same about of load (total force) like other material. Also, the stainless-steel has a better factor of safety at water depth of 1000m which is crucial to material selection.

3.2 Solid works analysis

Solid works analysis was performed on stainless-steel material simply because it was the material selected from all the water depth under consideration (1000m). Also, it offered us another alternative in determining the behaviour of the material under pressure. Since the only closed body of the ROV is the 4" section of PVC with the clear acrylic dome, this would be the only area experiencing hydrostatic pressure. The area under analysis is shown in the figure 9 below.

Figure 9 is the ROV frame diagram without load. The ROV frame acts as the main surface or area upon which the external forces will act and the beams are structural elements that primarily resist load-induced deformation, while the trusses provide support to the structure main frame. This analysis shows that without an imposed load, no part of the ROV frame is under any noticeable stress.

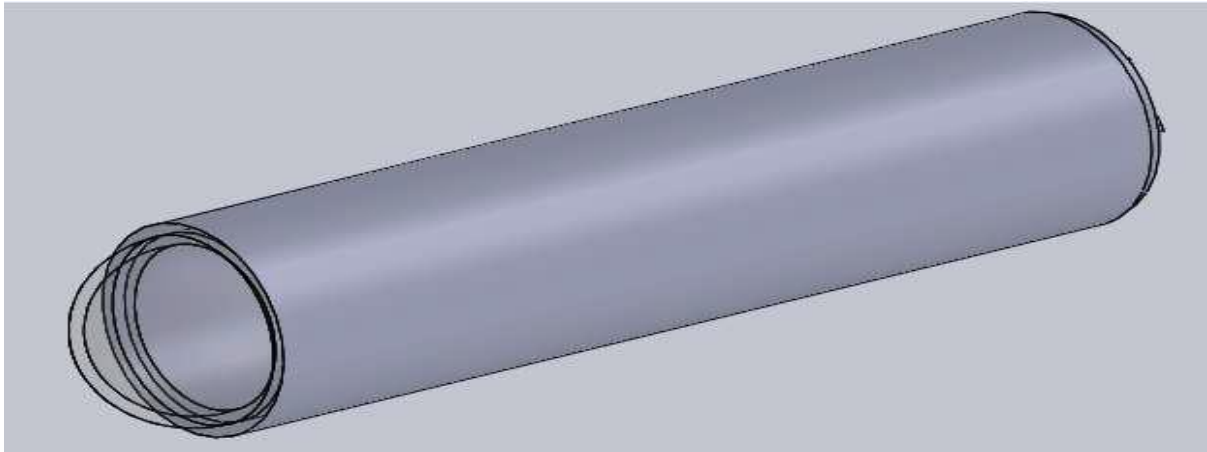


Figure 9: Frame Solid Work Analysis using Stainless-Steel

Figure 10 is the ROV frame self-weight diagram and hydrostatics load distribution per area on the stainless-steel material. This diagram further shows how the Program evenly distributed the imposed loads on the structure across the surface. However, the areas of the ROV frame that have direct contact with water flow are assumed to have more impact load and they are regarded as the danger zones.

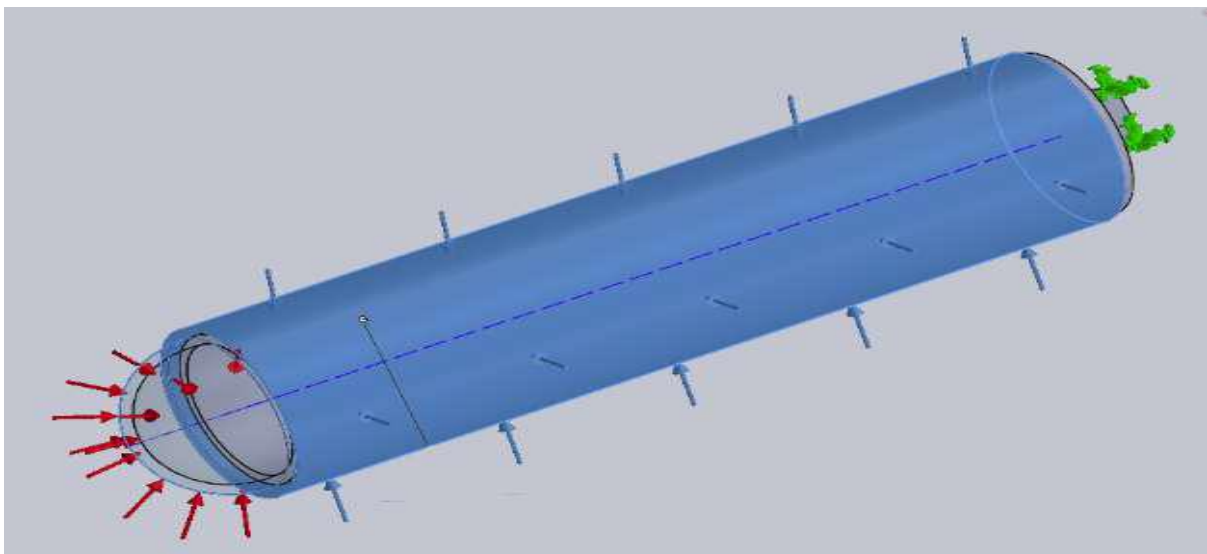


Figure 10: Location of the Hydrostatic Forces on the Frame of the ROV using Stainless-Steel

Figure 11 is the von mises stress of the ROV frame using Staa.Pro. Von mises are a failure criterion of structures under load which is the value used to determine if a given material will yield or fracture under load. The ROV frame under load which is the value used to determine if a given material will yield or fracture under load, and the important of this diagram is that it help to show if the stainless-steel material will fail under the different impacted load on the ROV frame based on the nodal sub-region employ, and the areas or region with least impacted load as shown on the diagram with blue coloration having a von mises stress less than 200466.5N/m^2 while the area or region with the most load impact or distribution is shown with red coloration with maximum von mises stress greater than or equal to 53936212N/m^2 .

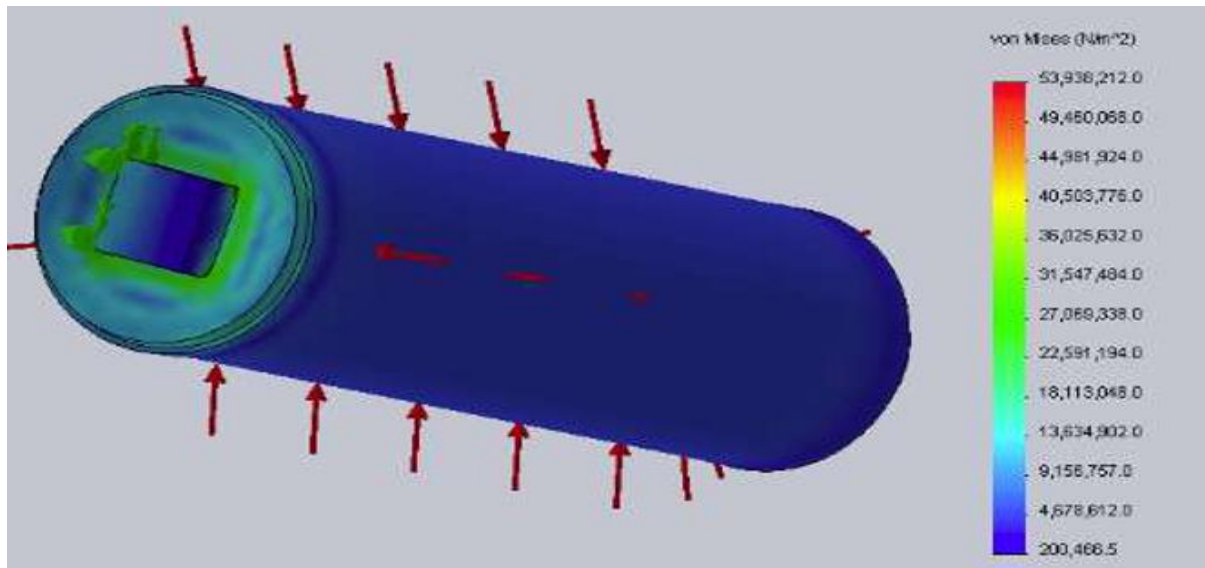


Figure 11: Von-mises Stress on the Frame of the ROV using Stainless-Steel

Figure 12 is the maximum internal displacement of the ROV frame. As seen in the images below, the inner cylinder frame that houses all the components is able to withstand over $50,000 \text{ N/m}^2$ with an inner displacement of 5mm as shown.

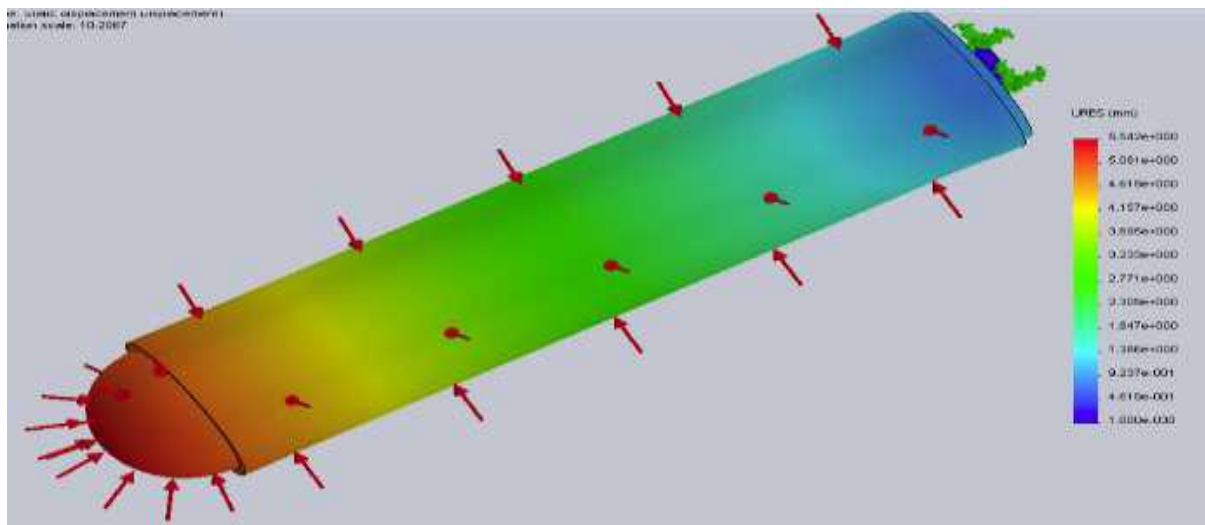


Figure 12: Maximum Internal Displacement on the Frame of the ROV using Stainless-Steel

3.3 Materials cost analysis

With the factor of safety calculations done, the attention was turned to the cost analysis. Due to the fact that each material is sold with a certain diameter, the cost of the material depends solely on its length. Keeping in mind that all models accounted for have the same length, it can be said that price will not change with the depth at which the specimen is sent. The prices were placed side by side with the maximum depth each material reached. In doing this, the material that went the deepest for the least amount of the cost would be the one selected.

Finally, with everything taken into consideration, the material that has the lowest cost and with the best Depth to Cost Ratio was selected. Taking the lowest depth achieved and dividing it by the price of the material calculate with the Depth to Cost Ratio. Of course, the higher the ratio the better the selection was. PVC Schedule 40 has the highest depth to cost ratio, although having a price that was slightly below that of PVC Schedule 40 will be accepted so long it meant the initial condition of 1.5 factor of safety at that water depth. had a better Depth to Cost Ratio. This means PVC Schedule 40 reached a depth of 1000 meters with the least depth to cost ratio while the stainless steel 316 reached same 1000 meters water depth with the highest depth to cost ratio as shown in table 2. In conclusion, the best material when considering depth to cost ratio are the PVC Schedule, though it is not enough to choose a material based on cost alone.

Table 2: Depth to Cost Analysis

ROV Frame Material Type	Percent of Budget	Depth to Cost Ratio
PVC Schedule 40	18.78%	43.48
PVC Schedule 80	15.44%	35.71
Aluminum 7075	20.13%	33.33
Titanium Grade 5	21.15%	31.25
Stainless Steel 316	24.49%	27.78

Table3 shows the Factor of Safety (FOS) of the different materials under study at varying Ocean depth. This table indicate the FOS at each water depth, it was observed that when table 3 was compared with table 2 the FOS move in the inverse of the Cost to Depth ratio. Meaning material with the highest cost to depth ratio (PVC Schedule 40) will have the lowest FOS at each water depth, also material with the lowest cost to depth ratio (Stainless Steel 317) will have the highest FOS at each water depth.

Table 3: Factor of Safety at Varying Ocean Depth

PVC Sch. 40		PVC Sch. 80		Aluminium 7075		Titanium Grade 5		Stainless Steel 316	
Depth	FOS	Depth	FOS	Depth	FOS	Depth	FOS	Depth	FOS
50m	0.800	50m	0.950	50m	1.050	50m	1.085	50m	1.107
100m	0.801	100m	0.980	100m	1.060	100m	1.095	100m	1.109
200m	0.805	200m	1.000	200m	1.120	200m	1.126	200m	1.130
300m	0.810	300m	1.005	300m	1.150	300m	1.159	300m	1.189
400m	0.815	400m	1.010	400m	1.180	400m	1.200	400m	1.255
500m	0.820	500m	1.100	500m	1.200	500m	1.254	500m	1.300
600m	0.830	600m	1.120	600m	1.285	600m	1.400	600m	1.516
700m	0.840	700m	1.140	700m	1.400	700m	1.780	700m	1.801
800m	0.850	800m	1.160	800m	1.580	800m	1.924	800m	2.010
900m	0.870	900m	1.180	900m	1.675	900m	2.145	900m	2.310
1000m	0.890	1000m	1.200	1000m	1.740	1000m	2.300	1000m	2.500

The task was to determine how deep into ocean the Remotely Operated Underwater Vehicle can dive while maintaining a safety factor of 1.5, and additionally figure 13 shows which material would allow us to achieve this goal with the best cost. The different materials will be tested according to the factor of safety in reference to the arbitrary of 1.5 factor of safety. It is to be noted that this is a simplified version of the actual model, which will be used as a preliminary analysis in order to understand the effects of hydrostatic pressures on an object under water. The model being analysis has a cylindrical body that is hollow inside. This will assimilate the body of the actual ROV without the two wing-like components of the model.

The ROV has a length of 1.2 meters and a diameter of 0.02 meters consistent with the real model. These measurements were kept the same for all the materials being tested and the only measurement that was changed was the thickness due to the fact that each material is sold with a certain thickness. The materials tested were PVC Schedule 40, PVC Schedule 80, Aluminium 7075, Stainless Steel 316 and Titanium (Grade 5). In order to measure the factor of safety of the ROV to ensure that the material will not fail regardless of water depth. Figure 4.26 shows the factor of safety against varying water depth. Each materials factor of safety was plotted against water depth and it was observed that the stainless steel 316 has highest factor of safety across the water depth. Also, the materials that meet the 1.5 factor of safety criteria are stainless steel 316, Titanium Grade 5 and Aluminum 7075. The PVC Schedule despite having the lowest depth to cost ratio fail to meet the 1.5 factor of safety condition as such could not be considered for selection or recommendation.

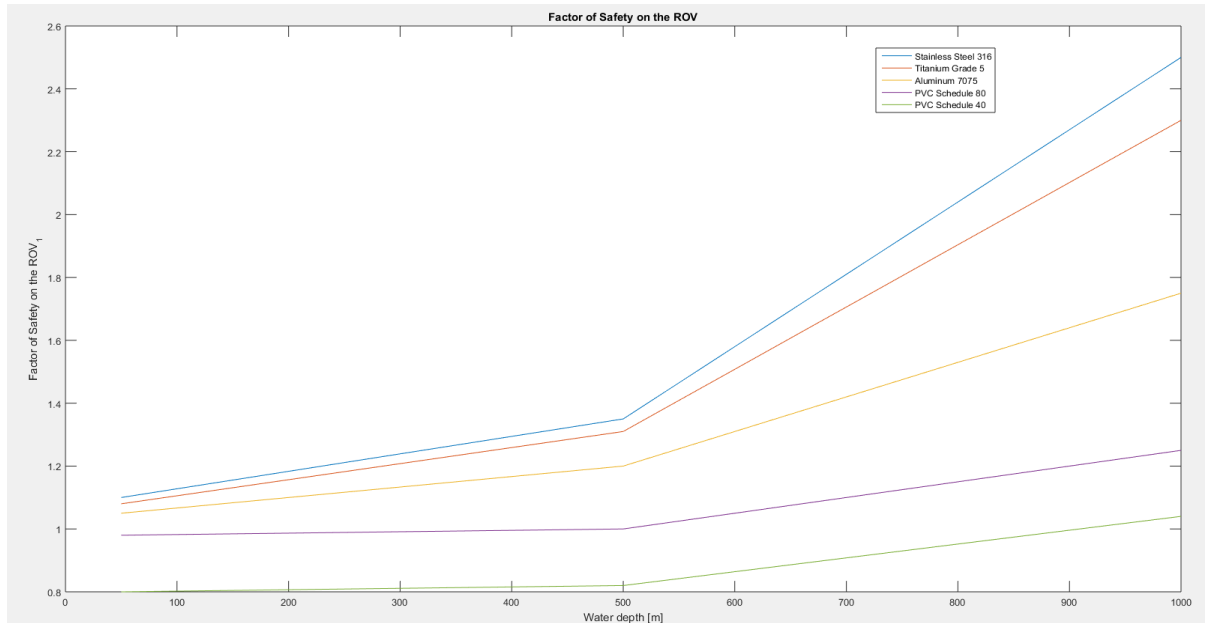


Figure 13: Factor of Safety of Different Materials in Comparison to Depth

IV. CONCLUSION

The aim of this dissertation was to select an appropriate material for the design of an ROV from five different material under study. In order for the dissertation to be successful, all the ROV frame material type are subjected to computational axial stress, principal stress and von-mises before a commercial software (Staad.Pro) was use to analysis the stress on the selected material.

The maximum internal displacement of the ROV frame that houses all the components is able to withstand over $50,000 \text{ N}/\text{m}^2$ with an inner displacement of 5mm as shown in figure 4.25. The result when compared with the maximum allowable stress of steel of 210 Mpa was found to be satisfactory.

The von mises stress of the ROV frame under load which is the value used to determine if a given material will yield or fracture under load was also computed during the ROV design. The von mises stress help to show if the material will fail under the different impacted load on the ROV frame based on the nodal sub-region employ, and the areas or region with least impacted load as shown in figure 4.24 with blue coloration having a von mises stress less than $200466.5 \text{ N}/\text{mm}^2$ while the area or region with the most load impact or distribution is shown with red coloration with maximum von mises stress greater than or equal to $53936212 \text{ N}/\text{mm}^2$.

The design also computes the power required to drive the ROV, the power that will be require to drive the ROV though the maximum power of about 2000kw at 1000meter water depth is the working power of the ROV for stainless steel which will require the highest power. It was also observed that the minimum drive power of the ROV (250kw) at different water depth was recorded at the point when the ROV is idle (time zero).

It can be concluded that water depth influences the total wave force, total force and power required by the ROV. The different in values between results of different materials are tend towards the maximum value as the water depth increases. At water depth 50meters the power required is 990kw to 700kw, as water depth increases to 500meters the power required is 1700kw to 1300kw and as water depth increases to 1000meters the power required is 2000kw to 1500kw. So, it is on the above note that the stainless-steel materials were chosen as an increase in water do not required much power require to drive the ROV.

Also, it can be concluded that the stainless steel is better suited for the ROV (when different ranges of depth are considered) than the other materials, because for both low and high depth, the factor of safety ranges from 1.1 to 2.5 for water depth range of (50meters to 1000meters) which is lesser than the factor of safety employ for other materials at 1.5. The other two material Titanium Grade 5 and Aluminum 7075 material can only be deployed when the water depth is about 1000meters, as it was at such water depth; the ROV has close values.

During this dissertation, some problems appeared. Most of them were solved, but not all of them. Therefore, the dissertation has a lot of space for further improvements. Even though the ROV does not have all intended features implemented, the system is functional at this point. Therefore, the main goal, material selection analysis for the design of a remotely operated vehicle, can be considered as accomplished.

References

- Ahmed, Y.M., Yaakob, O. & Sun, B.K., (2014). "Design of a new low cost ROV vehicle", *Journal of Technology*, 69(7), 1–11.
- Amudha, K., Rajesh, S., Ramesh, N.R., MuthukrishnaBabu, S., Abraham, R., Deepak, C.R. et al. (2009). Proceedings of the eighth, ISOPE ocean mining symposium, International Society of Offshore and Polar Engineering (ISOPE), China, 233–238.

-
- Guangyi, Z., Qingjun, Z., Zhiyu, Z., Xiaoqiang, D. & Chunlei, Z., (2018). "Research on underwater safety inspection and operational robot motion control", *33rd Youth Academic Annual Conference of Chinese Association of Automation (YAC) IEEE*, 322–327.
- Hasan, H., Rivai L.H.A., Iskandar, Y. & Claudio, P., (2018). "Design of Omni Directional Remotely Operated Vehicle (ROV)", *Journal of Physics: Conference Series*, 962(1), 12–17.
- Henri, B., Truls, N. & Terene, H., (2010). Petroleum and Chemical Industry Committee, IEEE, US, 1–9. International Electro technical Commission, IEC 61511-Part1. (2003). Switzerland: International Electro technical Commission. 1–48.
- International Standard IEC61511-Part3. (2003). Switzerland: International Electro technical Commission, 1–60.
- Manecius, S., Ramesh, R., Subramanian, A.N., Sathianarayanan, D., Harikrishnan, G., Jayakumar, V.K., et al. (2010). Twentieth International Offshore (Ocean) and Polar Engineering Conference, International Society of Offshore and Polar Engineering (ISOPE), Beijing, China, 206–212.
- Ramesh, R., Jayakumar, V.K., Manecius, S.J., DossPrakash, V., Ramadass, G.A., & Atmanand, M.A., (2010). 7th International Conference on Computational Intelligence, Robotics and Autonomous Systems (CIRAS) in 13th FIRA Robot World congress, FIRA 2010, New York, Springer-Verlag, Berlin Heidelberg, 33–40.
- Roy, K.L., (1998). Control of a Tethered Underwater Flight Vehicle, Ph.D thesis, University of Southampton.
- Salleh M.S.M. (2008). "Remotely Operated Underwater Vehicle (ROUV)", *Universiti Teknologi Malaysia*.
- Smith, D.J. & Simpson, K.G.L., (2010). Functional Safety – A Straight forward guide to applying IEC 61508 and related standards, Elsevier, UK, 280-285.
- Symes, K., (2013). Underwater Technology magazine, Society of Underwater Technology, London, 28–29.
- Vedachalam, N., Ramesh, R., Ramesh, S., Sathianarayanan, D., Subramaniam, A.N., Harikrishnan, G., et al. (2013). in: Proceedings of International symposium on Underwater Technology, IEEE, US, 1–10.